

# Universality in tightly bound 3-boson systems

Y. Z. He<sup>2</sup>, Y. Z. Fang<sup>2</sup>, and C. G. Bao<sup>1,2,\*</sup>

<sup>1</sup>*Center of Theoretical Nuclear Physics, National Laboratory of Heavy Ion Accelerator, Lanzhou, 730000, People's Republic of China and*

<sup>2</sup>*State Key Laboratory of Optoelectronic Materials and Technologies, School of Physics and Engineering, Sun Yat-Sen University, Guangzhou, 510275, People's Republic of China*

The effects of two distinct operations of the elements of the symmetry groups of a Hamiltonian on a quantum state might be equivalent in some specific zones of coordinate space. Making use of the matrix representations of the groups, the equivalence leads to a set of homogeneous linear equations imposing on the wave functions. When the matrix of the equations is non-degenerate, the wave functions will appear as nodal surfaces in these zones. Therefore, the equivalence leads to the existence of inherent nodal structure in the quantum states. In this paper, trapped 3-boson systems with different types of interactions are studied. The structures of the tightly bound eigenstates have been analyzed systematically. The emphasis is placed to demonstrate the universality arising from the common inherent nodal structures.

PACS numbers: 03.65.-w, 03.65.Ge, 02.20.-a, 21.45.-v, 36.40.Mr

## A. Introduction

It is well known that universality exists in weakly bound 3-body system, where the Efimov states emerge.[1, 2] These states arise from the inherent mysteries of quantum mechanics, and they are governed by a universal law, not depend on the details of dynamics. In this paper, another kind of universality that exists in tightly bound quantum mechanic few-body systems is revealed and confirmed numerically.

Usually, the Hamiltonian of identical particles is invariant under the operations of a set of symmetry groups  $G_\alpha, G_\beta, \dots$  (including the permutation group).[3–6] Consequently, the eigenstates  $\{\Psi_i(X)\}$  are classified according to the representations of these groups, where  $X$  denotes a set of coordinates and  $i$  is a serial number. Let  $g_\alpha$  be an element of  $G_\alpha$ ,  $g_\beta$  be that of  $G_\beta$  (each of them may be an element of the direct product of groups), and  $\Xi$  denotes a special zone in the high-dimensional coordinate space. When  $X \in \Xi$ , the operations of  $g_\alpha$  and  $g_\beta$  might be equivalent so that  $g_\alpha\Psi_i(X) = g_\beta\Psi_i(X)$ . For an example, when  $\Xi$  is the zone of regular triangles (RT),  $g_\alpha$  is the rotation about the normal of the triangle by  $2\pi/3$ , and  $g_\beta$  is a cyclic permutation of particles, then  $g_\alpha$  and  $g_\beta$  are equivalent in  $\Xi$ . Making use of the representations of groups, the equivalence leads to the establishment of a set of homogeneous linear equations  $\sum_{i'} [D_{i'i}^\alpha(g_\alpha) - D_{i'i}^\beta(g_\beta)]\Psi_{i'}(X) = 0$  in  $\Xi$ , where  $D_{i'i}^\alpha(g_\alpha)$  is the matrix element of the representation. When the matrix of this set of equations is non-degenerate, the set  $\Psi_i(X)$  must be zero in  $\Xi$ . In this case,  $\Xi$  becomes a prohibited zone and the wave function appears as an inherent nodal surface (INS).[7] Since the matrixes of representations are absolutely irrelevant to dynamics, the appearance of the INS is universal disregarding the kind

of systems (nuclear, atomic, or molecular) and the details of dynamic parameters.

The inherent nodal structures of 3-boson systems (without a trap) has been studied by the authors previously.[8, 9] Accordingly, the quantum states can be naturally classified according to their inherent nodal structures.[8–11] Due to the progress of techniques, a few atoms can be tightly bound in a magnetic or optical trap. Thus the study of these systems is meaningful. The present paper extends the previous research of the authors and is dedicated to trapped 3-body systems. A more effective and simpler approach is proposed for the analysis. In particular, in addition to the RT, the symmetry constraint associated with the isosceles triangle (IST) and the collinear geometry (COL) has also been taken into account. By studying the spectra, the root mean square radii, the particle spatial distribution, the weights of  $Q$ -components ( $Q$  is the projection of the total orbital angular momentum  $L$  on the third body-axis), and the shape-densities, systematic knowledge on the quantum states has been obtained. The emphasis is placed on demonstrating the universality by comparing different 3-boson systems. In addition to boson systems, a short discussion on fermion systems is also given at the end.

## B. Hamiltonian, spectra, and the eigen-states

It is assumed that the three particles are confined by an isotropic harmonic trap  $\frac{1}{2}m\omega^2r_i^2$ . Due to the trap numerous bound states exist, therefore a systematic analysis can be made.  $\hbar\omega$  and  $\sqrt{\hbar/m\omega}$  are used as units of energy and length. Three types of interactions are assumed:  $V_A(r) = 10(2e^{-(r/1.428)^2} - e^{-(r/2.105)^2})$ ,  $V_B(r) = 1000e^{-3r} - 40/r^6$  ( $r \geq 1.2$ ) and  $V_B(r) = V_B(1.2)$  ( $r < 1.2$ ), and  $V_C(r) = 0$  ( $r \geq 1$ ) and  $V_C(r) = 15$  ( $r < 1$ ). The type  $V_A$  has a short-ranged character and was previously used in nuclear physics for the  $\alpha$ -particles,  $V_B$

\*Corresponding author: stsbcg@mail.sysu.edu.cn

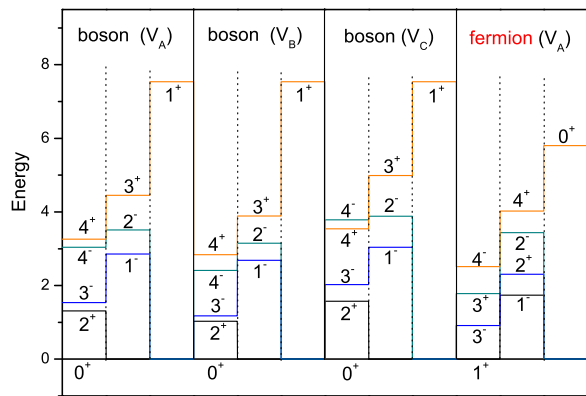


FIG. 1: Spectra of 3-body systems with  $L = 0$  to 4 and parity  $\Pi = \pm 1$ . Only the first-states are involved. For bosons three types of interactions  $V_A$ ,  $V_B$ , and  $V_C$  are considered. For fermions (the spatial wave functions are totally antisymmetric) only  $V_A$  is considered. The levels have been shifted so that all the ground states have energy zero. The energy unit for the two cases with  $V_A$  is  $\hbar\omega$ . In the case with  $V_B$  or  $V_C$  the energy unit has been redefined so that the energy of the  $1^+$  state has the same value as the one with  $V_A$ . In every case the states are divided into three groups. For bosons, when different interactions are used the members and sequence in each group are the same (the only exception is that  $4^-$  is higher than  $4^+$  when  $V_C$  is used).

belongs to the Van der Waals type for atoms, while  $V_C$  is just a hard core potential. In fact, the interactions are chosen quite arbitrary, just to show the inherent universality among different systems. The Hamiltonian is

$$H = \sum_i \left( -\frac{1}{2} \nabla_i^2 + \frac{1}{2} r_i^2 \right) + \sum_{i < j} V_J(|\mathbf{r}_i - \mathbf{r}_j|), \quad (1)$$

$(J = A, B, \text{ or } C).$

A set of basis functions is introduced to diagonalize the Hamiltonian to obtain the spectra and the eigenstates. The details are given in the appendix. Note that both  $V_A$  and  $V_B$  contain a minimum, and therefore the low-lying states will pursue a better geometry so that the particles are appropriately separated and the total potential energy can be thereby lower. This pursuit is not obvious for the case with  $V_C$ , where no minimum is contained.

When the c.m. motion is removed an eigenstate is denoted as  $\Psi_{L,M}^{\Pi,i}$ , where  $M$  is the  $Z$ -component of  $L$ ,  $\Pi$  the parity, and  $i$  denotes the  $i$ -th state of a  $L^\Pi$ -series. The  $i = 1$  state (the lowest in a series) is called a first-state. The label  $i$  is usually ignored when  $i = 1$ . For the three types of interaction the spectra of nine first-states are plotted in Fig. 1 (the  $L^\Pi = 0^-$  state does not exist due to the "Rule 1" given below), where the spectrum at the right is for fermions and will be concerned later. It turns out that the three spectra at the left for bosons are similar. The levels can be similarly divided into three groups. In a group, the structures of the states are similar as shown below, and those with a larger  $L$  are higher due

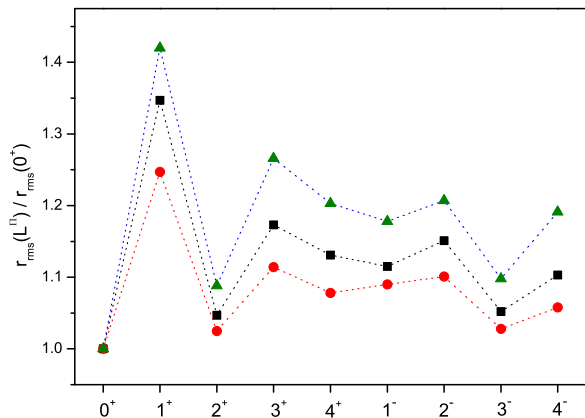


FIG. 2: The ratio  $r_{\text{rms}}(L^\Pi)/r_{\text{rms}}(0^+)$ , of the  $L^\Pi$  states. Square is for  $V_A$ , circle for  $V_B$ , and triangle for  $V_C$ .

to the rotation energy. Many common features existing in the three spectra (say,  $1^+$  is particularly high,  $3^+$  is much higher than  $3^-$ , and  $2^-$  is much higher than  $2^+$ , etc.) can not be explained simply by dynamics. It implies the existence of a more fundamental reason.

The root mean square radius  $r_{\text{rms}}(L^\Pi)$  is extracted from  $\Psi_{L,M}^\Pi$  to evaluate the size. The ratios  $r_{\text{rms}}(L^\Pi)/r_{\text{rms}}(0^+)$  are shown in Fig. 2 where the three dotted lines guiding the eyes go up and down in a synchronous way. For all the three types of interactions, the sizes of  $0^+$ ,  $2^+$ , and  $3^-$  are relatively smaller, while the sizes of  $1^+$  is the largest. From dynamics, the  $4^+$  and  $4^-$  states are expected to be larger in size because the particles are pushing out by a stronger centrifugal force, but in fact not. It demonstrates again the existence of a more fundamental reason.

Let  $\mathbf{k}'$  be a unit vector vertical to the plane of particles. For  $L \neq 0$  states, the relative orientation of  $\mathbf{k}'$  and  $L$  is a noticeable feature. Let a body frame  $\Sigma'$  with the base-vectors  $\mathbf{i}' - \mathbf{j}' - \mathbf{k}'$  be introduced, where  $\mathbf{j}'$  lies along  $\mathbf{R} \equiv \mathbf{r}_3 - (\mathbf{r}_1 + \mathbf{r}_2)/2$ . Then, the eigenstates can be expressed as  $\Psi_{LM}^\Pi(X) = \sum_Q D_{QM}^L(\Omega) \Psi_{LQ}^\Pi(X')$  where  $X$  denotes the set of coordinates relative to a fixed frame  $\Sigma$ , and  $X'$  denotes the set relative to  $\Sigma'$ ,  $\Omega$  denotes the three Euler angles responsible for the transformation from  $\Sigma'$  to  $\Sigma$ . [12] Starting from the normality  $1 = \langle \Psi_{L,M}^\Pi | \Psi_{L,M}^\Pi \rangle$ , we carry out first the integration over  $\Omega$ . Then we have

$$1 = \sum_Q \frac{8\pi^2}{2L+1} \int dX' |\Psi_{L,Q}^\Pi(X')|^2 \equiv \sum_Q W_Q, \quad (2)$$

where  $dX'^2 = R^2 dr dR \sin \theta d\theta$ ,  $\theta$  is the angle between  $\mathbf{r} \equiv \mathbf{r}_2 - \mathbf{r}_1$  and  $\mathbf{R}$ .  $W_Q$  is the weight of the  $Q$ -component  $\Psi_{LQ}^\Pi$ . Note that  $Q$  is the projection of  $L$  along  $\mathbf{k}'$ . Thus, in  $\Psi_{LL}^\Pi$ ,  $L$  is essentially lying along  $\mathbf{k}'$  and therefore is essentially vertical to the plane of particles. Whereas in  $\Psi_{L0}^\Pi$ ,  $L$  is essentially lying on the  $\mathbf{i}' - \mathbf{j}'$  plane and therefore is coplanar with the particles. Thus, the relative orientation between  $L$  and  $\mathbf{k}'$  can be understood from  $W_Q$ .

Carrying out the integration over  $dX'$  numerically,  $W_Q$  can be obtained. Since  $W_Q = W_{-Q}$ , we define  $\bar{W}_Q = 2W_Q$  (if  $Q \neq 0$ ), or  $= W_Q$  (if  $Q = 0$ ). They are given in Tab. I.

TABLE I: The weights of the  $|Q|$ -components obtained by using  $V_A$ .

	$\bar{W}_0$	$\bar{W}_1$	$\bar{W}_2$	$\bar{W}_3$	$\bar{W}_4$
$0^+$	1				
$1^+$	1				
$2^+$	0.862		0.138		
$3^+$	0.001		0.999		
$4^+$	0.529		0.305		0.166
$1^-$		1			
$2^-$		1			
$3^-$		0.016		0.984	
$4^-$		0.016		0.929	

$\bar{W}_Q$  are far from uniform but concentrated in one  $|Q|$ -component (except in  $4^+$ ). When other interactions are used the qualitative features of  $\bar{W}_Q$  remain unchanged (say, for  $V_A, V_B$  and  $V_C$ , respectively,  $3^-$  has  $\bar{W}_3 = 0.984, 0.991$ , and  $0.972$ ). Thus, again, there is a fundamental reason beyond dynamics.

### C. Symmetry constraint and the classification of states

To clarify the fundamental reason, we study the effect of equivalent operations. Let the operator of a rotation about an axis  $\mathbf{a}$  by an angle  $\beta$  be denoted as  $\mathcal{R}_\beta^{\mathbf{a}}$ . When  $\mathbf{a}$  is  $\mathbf{k}'$  which is vertical to the plane of particles, the rotation by  $\pi$  is equivalent to an inversion  $\mathcal{I}$  with respect to the c.m.. Thus we have  $\mathcal{R}_\pi^{\mathbf{k}'} \Psi_{LQ}^\Pi = e^{-i\pi Q} \Psi_{LQ}^\Pi = \Pi \Psi_{LQ}^\Pi$ . It leads to the "Rule 1: *only  $Q$  even (odd) components are allowed for parity even (odd) states*" as shown in the table. Furthermore, at a RT,  $\mathcal{R}_{2\pi/3}^{\mathbf{k}'} \Psi_{LQ}^\Pi = e^{-i\frac{2\pi}{3}Q} \Psi_{LQ}^\Pi = P_{\text{cyc}} \Psi_{LQ}^\Pi$ , where  $P_{\text{cyc}}$  denotes a cyclic permutation of particles and will cause no effect. Thus, we have the "Rule 2:  $\Psi_{L,Q}^\Pi$  is nonzero at a RT only if  $Q = 0, \pm 3, \pm 6, \dots$ ". When the three particles turn out to form an IST (including the RT as a special case) with the symmetric axis  $\mathbf{v}$  lying on the  $\mathbf{i}'\text{-}\mathbf{j}'$  plane, we have the equivalence  $\mathcal{R}_\pi^{\mathbf{v}} \Psi_{LQ}^\Pi = P_{ij} \Psi_{LQ}^\Pi$ , where  $P_{ij}$  denotes the interchange of the two particles at the bottom of the IST. It leads to  $e^{-i2\delta Q} (-1)^{L+Q} \Psi_{L,-Q}^\Pi = \varepsilon \Psi_{LQ}^\Pi$ , where  $\delta$  is the angle between  $\mathbf{v}$  and  $\mathbf{j}'$ , and  $\varepsilon = \pm 1$  depends on the statistics. Thus, for bosons and for  $Q = 0$ , we have the "Rule 3:  $\Psi_{L,0}^\Pi$  is nonzero at an IST only if  $L$  is even". With the three rules, when  $L \leq 4$ , the RT-accessible components are  $\Psi_{L=\text{even},0}^{\Pi=1}$  and  $\Psi_{L=\text{odd},\pm 3}^{\Pi=-1}$ .

Since all the three bonds can be optimized in a RT, the RT-accessible (RT-ac) components are much favored

by the lower states. Among the nine states under consideration, the RT-ac components can be contained in the  $0^+, 2^+, 4^+, 3^-$  and  $4^-$  states. They are called the RT-ac states and are dominated by the RT-ac component with  $|Q| = 0$  (3) if  $\Pi = 1$  ( $-1$ ) (as shown in Table 1), thereby their energies can be much lower and they constitute the lowest group in the spectrum. Their wave functions are distributed surrounding a RT resulting in having a smaller size. The domination of the RT-ac component explains why  $\bar{W}_0$  or  $\bar{W}_3$  is particularly large in the RT-ac states.

For  $1^+$ , the  $|Q| = 1$  component is prohibited by "Rule 1", while in the  $Q = 0$  component the IST is prohibited by "Rule 3". The prohibition of all the IST causes serious consequence. It implies that the wave function is expelled from the important zones of coordinate space (see below) resulting in having a very high energy and a large size. This explains why this state belongs to the highest group in the spectra.

For  $1^-$  and  $2^-$ , only  $|Q| = 1$  is allowed due to "Rule 1". This component is IST-ac but RT-inaccessible (RT-inac). Accordingly, these states are classified to the second group. For  $3^+$ , both  $|Q| = 0$  and 2 components are allowed. Due to "Rule 3", the former is IST-inac and therefore extremely unfavorable. Thus the weights are greatly concentrated in  $\bar{W}_2$  as shown in Table 1. Since the  $|Q| = 2$  component is also IST-ac and RT-inac,  $3^+$  belongs also to the second group.

Since the classification is based on the accessibility of the RT and IST originating from symmetry constraint, it is universal for all kinds of 3-boson systems.

### D. One-body densities

Since the weights  $\bar{W}_Q$  are related to the relative orientation between  $\mathbf{k}'$  and  $L$ , these weights are related to the one-body densities  $\rho_1$  which is an observable. Let us go back to the fixed-frame and deal with the eigenstates  $\Psi_{LM}^\Pi(\mathbf{r}, \mathbf{R})$ . From the normality, we have

$$1 = \int d\mathbf{r} d\mathbf{R} |\Psi_{LM}^\Pi|^2 \equiv \int d\mathbf{r}_3 \rho_1(\mathbf{r}_3), \quad (3)$$

where  $\mathbf{r}_3 = \frac{2}{3}\mathbf{R}$  is the position vector of the third particle relative to the c.m., and  $3\rho_1(\mathbf{r}_3)$  is the probability density of finding a particle (disregarding which one) at  $\mathbf{r}_3$ . Let  $M = L$ , it implies that  $L$  is given along the  $Z$ -axis. The  $\rho_1$  extracted from  $\Psi_{LL}^\Pi$  is plotted in Fig. 3. For  $3^-$ , since this state is dominated by  $\bar{W}_3$ ,  $\mathbf{k}'$  is essentially lying along  $L$  (i.e., along the  $Z$ -axis at the choice  $M = L$ ). Therefore, it is expected that the  $\rho_1$  of  $3^-$  would be distributed close to the X-Y plane. This presumption is confirmed in Fig. 3. For  $4^-$ ,  $\bar{W}_3$  is also dominant, thus the direction of  $L$  is close to but deviates a little from the  $Z$ -axis. Accordingly, the peak of  $\rho_1$  of  $4^-$  is close to but deviates from  $\theta_3 = 90^\circ$ .  $3^+$  is dominated by  $\bar{W}_2$ . Accordingly, the peak is farther apart from  $90^\circ$ . Whereas

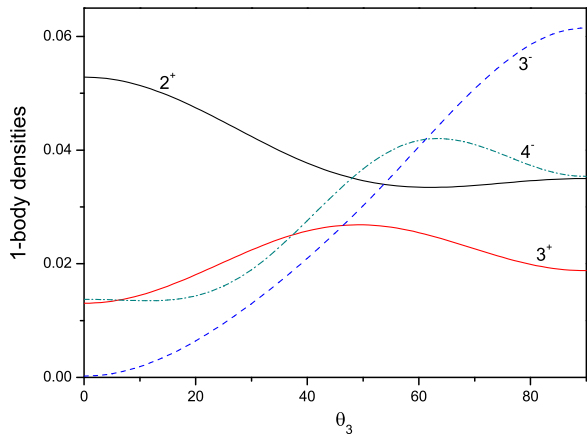


FIG. 3: One-body densities  $\rho_1(r_3, \theta_3)$  of the  $\Psi_{LL}^\Pi$  states calculated by using  $V_A$  and with  $r_3$  given at  $r_{\text{rms}}$ .  $\theta_3$  is the polar angle.  $\rho_1(r_3, \theta_3) = \rho_1(r_3, \pi - \theta_3)$ , and  $\rho_1$  does not depend on the azimuthal angle.

$2^+$  is dominated by  $\bar{W}_0$ . Therefore  $\mathbf{k}'$  is essentially vertical to the  $Z$ -axis, thus the plane of the particles prefer to be coplanar with the  $Z$ -axis if  $|M| = L$ , and the distribution is no more close to the equator. In fact, the  $\rho_1$  of  $2^+$  is peaked at  $\theta_3 = 0$ .

Although Fig. 3 is from  $V_A$ , the feature is common for various 3-boson systems. For examples, when  $V_A$ ,  $V_B$ , and  $V_C$  are used, the  $\rho_1$  of  $4^-$  is peaked at  $63^\circ$ ,  $63^\circ$ , and  $66^\circ$ , respectively, and the  $\rho_1$  of  $3^+$  is peaked at  $50^\circ$ ,  $49^\circ$ , and  $49^\circ$ .

### E. Shape-densities

Let us study the structures of the states in more detail in the body-frame. We define the hyper-radius  $\mathfrak{h} = \sqrt{\frac{1}{2}r^2 + \frac{2}{3}R^2}$ . This quantity is invariant under the transformation between different sets of Jacobi coordinates. Therefore, it is suitable to describe the size. Furthermore, we define  $\tan \beta = \sqrt{2/3}R/(\sqrt{1/2}r)$ . When  $r$  and  $R$  are replaced by  $\mathfrak{h}$  and  $\beta$  as arguments, Eq. (2) can be rewritten as

$$1 = \int d\mathfrak{h} dS \rho_{\text{sha}}(X'), \quad (4)$$

where  $dS = \frac{3\sqrt{3}}{(1+\tan^2\beta)(1+1/\tan^2\beta)} d\beta \sin\theta d\theta$  is an infinitesimal deformation, and

$$\rho_{\text{sha}}(X') = \frac{8\pi^2}{2L+1} \mathfrak{h}^5 \sum_Q |\Psi_{LQ}^\Pi(X')|^2, \quad (5)$$

is the probability density that the system has a given size and a given shape (while an integration over the orientation of the shape has already been carried out). Therefore  $\rho_{\text{sha}}(X')$  is called the shape-density which relates directly to the structure.

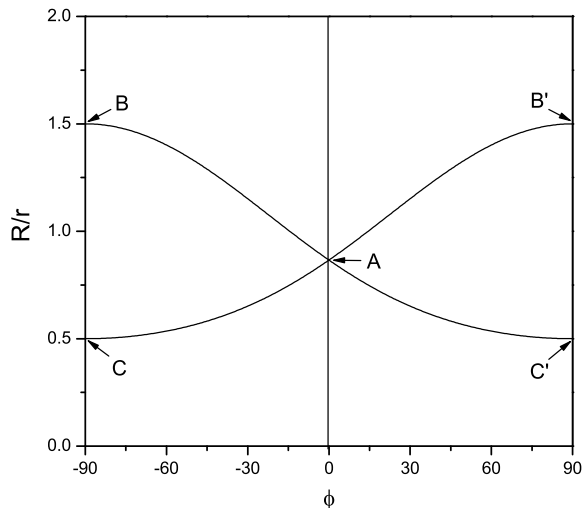


FIG. 4: Geometries in the  $(\phi, R/r)$  subspace. Where both the curves  $\widetilde{BAC'}$  and  $\widetilde{B'AC}$  correspond to the IST. These curves fulfill the equation  $R/r = \frac{1}{2}\sqrt{5-4F}$ , and  $F = \frac{1}{2}(\cos^2\phi \pm \sqrt{(3+\sin^2\phi)\sin^2\phi})$ . The vertical line  $\phi = 0$  corresponds also to the IST. The intersection  $A$  ( $\phi = 0, R/r = \sqrt{3}/2$ ) corresponds just to a RT. Both the vertical lines  $\phi = \pm 90^\circ$  correspond to collinear structures COL. In particular, the point  $B$  and  $B'$  together with the horizontal line  $R/r = 0$  correspond to a symmetric COL, namely, a particle sits at the middle of the other two. The point  $C$  and  $C'$  correspond also to a COL but with two particles overlap with each other.

Let  $\phi$  be the azimuthal angle of  $\mathbf{r}$  lying on the  $i'-j'$  plane. Since  $\mathbf{R}$  is given lying along  $\mathbf{j}'$ ,  $\phi = \pi/2 - \theta$ . Let  $\mathfrak{h}$  be given at  $\sqrt{3}r_{\text{rms}}$  (Let  $r_i$  be the distance of the  $i$ -th particle from the c.m.. Then  $\mathfrak{h} \equiv \sqrt{r_1^2 + r_2^2 + r_3^2}$ , and the average  $\bar{\mathfrak{h}} = \langle |r_1^2 + r_2^2 + r_3^2| \rangle^{1/2} = \sqrt{3}r_{\text{rms}}$ ). Examples of  $\rho_{\text{sha}}$  as a function of  $\phi$  and  $R/r \equiv \frac{\sqrt{3}}{2}\tan\beta$  are given below. The geometry associated with the arguments  $(\phi, R/r)$  is shown in Fig. 4.

When  $V_A$  is used, the  $\rho_{\text{sha}}$  of the RT-ac first-states are very similar with each other (except  $4^+$ ) as shown in Fig. 5a and 5b. The  $\rho_{\text{sha}}$  of  $4^+$  is shown in 5c. All of them are peaked at  $(\phi, R/r) = (0, \sqrt{3}/2)$  associated with a RT as expected. In 5c the peak is extended along three directions each leading to a COL. All the three RT-inac and IST-ac first-states are similar as shown in 5d, where a node appears at the RT and the three peaks are all associated with a flattened IST with particles 3, 1, and 2 at the top, respectively. The top angles of the IST are  $94^\circ$ ,  $101^\circ$ , and  $105^\circ$ , respectively for  $3^+$ ,  $1^-$ , and  $2^-$ . The  $\rho_{\text{sha}}$  of the IST-inac state  $1^+$  is shown in 5f, where a number of nodal lines exist in the  $(\phi, R/r)$  subspace, and the wave functions are expelled and compressed into six separate regions. The appearance of so many nodal lines implies the existence of a very strong inherent oscillation. This explains why  $1^+$  is very high in energy. From the different patterns of the  $\rho_{\text{sha}}$ , we know that the classification based on the accessibility of geometries is

valid.

For a COL, let  $\mathbf{k}'$  be set along the line of particles, then the rotation about  $\mathbf{k}'$  by any angle causes nothing. Hence the COL exists only in the  $Q = 0$  component (it implies that  $L$  is essentially vertical to  $\mathbf{k}'$ ). Besides, a rotation about  $\mathbf{j}'$  by  $\pi$  is equivalent to an inversion. This leads to  $(-1)^L \Psi_{L0}^\Pi = \Pi \Psi_{L0}^\Pi$ . Accordingly, only the states with  $(-1)^L = \Pi$  are allowed to have the COL. Furthermore, for a symmetric COL, an inversion is equivalent to an interchange of the two particles at the ends. Thus, the symmetric COL exists only in positive parity states (for bosons). When a COL is accessible but the symmetric COL is not, the COL is not stable because an inherent node is contained and a linear oscillation is inherently excited. On the other hand, from pure dynamics, a COL will have a larger moment of inertia. Comparing with the RT, a COL will have a higher interaction energy but a smaller rotation energy. Hence, this structure will be preferred by the states with a larger  $L$  so that the rotation energy can be considerably reduced. With this analysis, among the nine states, obviously, the COL will be more preferred by  $4^+$ . This explains the extension found in 5c, but not in 5a and 5b. It is expected that the COL will definitely appear in  $i \geq 2$  states as shown in 5e for  $4_2^+$ , where the most probable shape is a symmetric COL. Incidentally,  $1^+$  as shown in 5f is not only IST-inac but also COL-inac, this explains why so many nodal lines emerge.

When  $V_B$  is used, the qualitative features of Fig. 5 remain unchanged. Note that all the first states will do their best to pursue a structure favorable in binding and free from the symmetry constraint. This leads to the similarity. When  $V_C$  is used, the total potential energy is not sensitive to the details of geometry because the interaction does not contain a minimum. Hence, the pursuit to a better geometry is less anxious. This is shown in 6a (Comparing with 5d, the IST is no more well kept) and in 6b (where the distribution extends towards the COL. This tendency is not explicit in  $2_1^+$  if  $V_A$  or  $V_B$  is used).

## F. Fermion systems

For fermion systems, we consider the case that the spatial wave function is totally antisymmetric against particle permutation. Then the above Rule 1 and 2 hold exactly while Rule 3 becomes " $\Psi_{L,0}^\Pi$  is nonzero at an IST only if  $L$  is odd". With the three rules of fermions, when  $L \leq 4$ , the RT-ac states are  $1^+$ ,  $3^+$ ,  $3^-$ , and  $4^-$ . The RT-inac but IST-ac states are  $1^-$ ,  $2^+$ ,  $2^-$ , and  $4^+$ . The IST-inac state is  $0^+$ . The spectrum from numerical calculation by using  $V_A$  is shown at the right of Fig. 1, where the classification into three groups is revealed. As bosons, only the states with  $(-1)^L = \Pi$  are allowed to access the COL. However, the symmetric COL is accessible only to  $\Pi = -1$  states. From an analysis of the  $Q$ -components, we know that  $3^-$  has its RT lying on the  $i'-j'$  plane, while the RT of  $3^+$  is upstanding. Further-

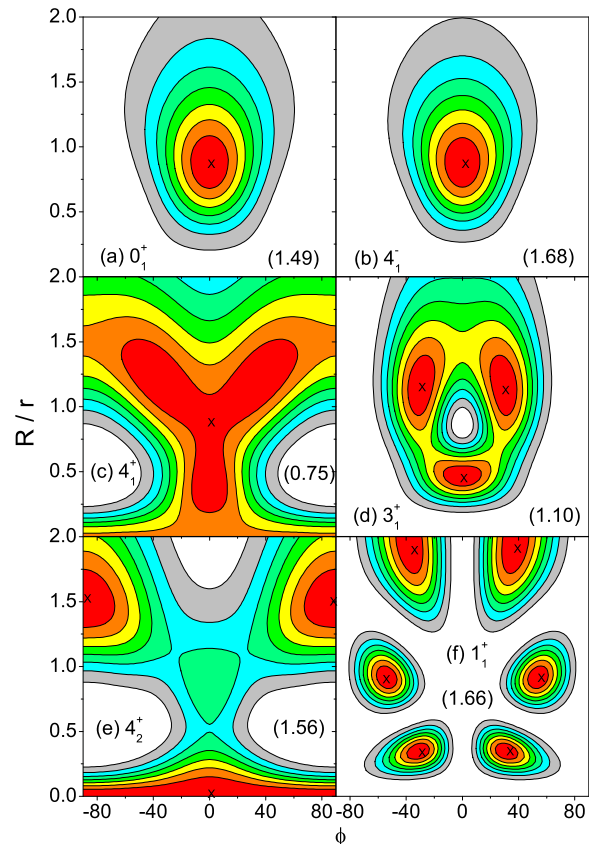


FIG. 5: The shape-densities  $\rho_{\text{sha}}$  of some selected  $L_1^\Pi$  first-states (an exception is 5e for the second-state) obtained by using  $V_A$ . For each state the hyper-radius  $\mathfrak{h}$  is given at  $\sqrt{3}r_{\text{rms}}$ , and the orientation of the shape has been integrated. The maxima of  $\rho_{\text{sha}}$  are marked by a cross and their values are given inside the parenthesis in each panel. The values of the contours form an arithmetic series and decrease to zero.

more  $3^-$  is symmetric-COL-ac, while  $3^+$  is not. This explains why  $3^-$  is lower than  $3^+$  even though they belong to the same group. Similarly, the IST in  $2^+$  is lying, that in  $2^-$  is not (due to the prohibition of  $Q$  even component). Besides,  $2^+$  is COL-ac while  $2^-$  is not. This explains why  $2^+$  is lower than  $2^-$  even though they belong to the same group.

Examples of  $\rho_{\text{sha}}$  of the 3-fermion states are shown in Fig. 6c and 6d. Fig. 6c is similar to 5f where the wave function is absolutely expelled from the lines of IST. However,  $0^+$  of fermions is COL-ac (but symmetric COL-inac) while  $1^+$  of bosons is not. Therefore, under the same interaction the  $0^+$  of fermions is lower (see Fig. 1), and its most probable shape is a non-symmetric COL with an inherent strong linear oscillation (due to the nodal lines). Comparing Fig. 6d and 5c (both for  $4^+$  but for fermions and bosons, respectively), the wave function of the former is expelled from the RT and also from the symmetric COL, while the latter is attracted by the COL. Thus the former is higher.

## Appendix

### I. DIAGONALIZATION OF THE HAMILTONIAN AND AN EVALUATION OF THE ACCURACY

When the c.m. coordinates have been removed, the Hamiltonian for internal motion  $H_{\text{int}}$  can be expressed by a set of Jacobi coordinates  $\mathbf{r} = \mathbf{r}_2 - \mathbf{r}_1$ , and  $\mathbf{R} = \mathbf{r}_3 - (\mathbf{r}_1 + \mathbf{r}_2)/2$ . Let

$$h(\mu, \mathbf{r}) \equiv -\frac{1}{2\mu}\nabla_{\mathbf{r}}^2 + \frac{1}{2}\mu r^2, \quad (6)$$

which is the Hamiltonian of harmonic oscillation, Then

$$H_{\text{int}} = h(1/2, \mathbf{r}) + h(2/3, \mathbf{R}) + \sum_{i<j} V(|\mathbf{r}_j - \mathbf{r}_i|). \quad (7)$$

Let us introduce a variational parameter  $\gamma$ . The eigenstates of  $h(\gamma, \mathbf{r})$  are denoted as  $\phi_{nl}^{\gamma}(\mathbf{r})$  with eigenenergy  $2n + l + 3/2$ , where  $n$  and  $l$  are the radial and angular quantum numbers, respectively. From  $\phi_{nl}^{\gamma}(\mathbf{r})$  a set of basis functions for the 3-body system is defined as

$$\Phi_{k,\Pi LM}^{\gamma}(123) \equiv (\phi_{n_a l_a}^{\gamma/2}(\mathbf{r}) \phi_{n_b l_b}^{2\gamma/3}(\mathbf{R}))_{LM}, \quad (8)$$

where  $l_a$  and  $l_b$  are coupled to the total orbital angular momentum  $L$  and its  $Z$ -component  $M$ ,  $\Pi = (-1)^{l_a+l_b}$  the parity,  $k$  denotes  $n_a, l_a, n_b,$  and  $l_b$ . These functions should be further (anti)symmetrized, thus we define

$$\tilde{\Phi}_{k,\Pi LM}^{\gamma} \equiv \sum_p \Phi_{k,\Pi LM}^{\gamma}(p_1 p_2 p_3), \quad (9)$$

where the right side is a summation over the permutations. Making use of the Talmi-Moshinsky coefficients, [13–15] each term at the right can be expanded in terms of  $\Phi_{k',\Pi LM}^{\gamma}(123)$ . Say,

$$\tilde{\Phi}_{k,\Pi LM}^{\gamma}(132) = \sum_{k'} A_{kk'}^{\Pi L} \Phi_{k',\Pi LM}^{\gamma}(123), \quad (10)$$

where the Talmi-Moshinsky coefficients  $A_{kk'}^{\Pi L}$  can be obtained by using the method given in the ref.[15]. Note that the set  $\{\tilde{\Phi}_{k,\Pi LM}^{\gamma}\}$  has not yet been orthonormalized. Thus a standard procedure is further needed to transform  $\{\tilde{\Phi}_{k,\Pi LM}^{\gamma}\}$  to a orthonormalized set  $\{\tilde{\tilde{\Phi}}_{q,\Pi LM}^{\gamma}\}$ , where  $q$  is a serial number. Each  $\tilde{\tilde{\Phi}}_{q,\Pi LM}^{\gamma}$  can be expanded in terms of  $\{\Phi_{k,\Pi LM}^{\gamma}(123)\}$ . Finally, the set  $\{\tilde{\tilde{\Phi}}_{q,\Pi LM}^{\gamma}\}$  is used to diagonalize  $H_{\text{int}}$ . Due to the symmetrization the matrix element of any pair of interaction is equal to that of the pair 1 and 2. Thus only  $\mathbf{r}$  and  $\mathbf{R}$  are involved in the calculation. This leads to a great convenience. When  $\Pi$  and  $L$  are given, a series of states will be obtained after the diagonalization. The lowest one of the series is called the first state. Its energy should be minimized by adjusting  $\gamma$ .

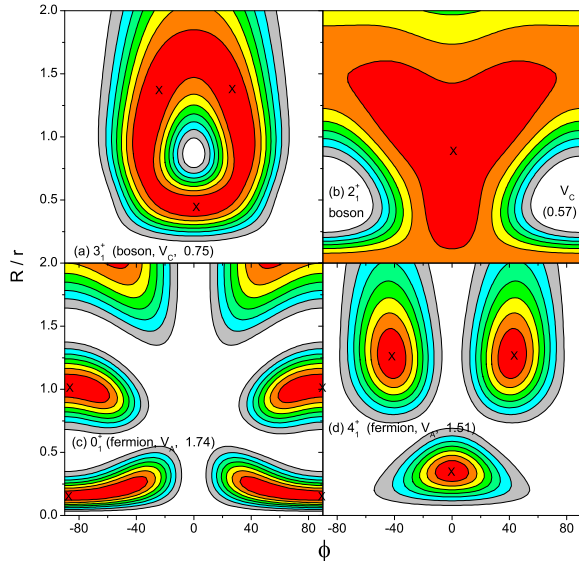


FIG. 6:  $\rho_{\text{sha}}$  obtained by using  $V_C$  for bosons (a and b), and  $\rho_{\text{sha}}$  obtained by using  $V_A$  for fermions (c and d). Refer to Fig. 5.

### G. Final remarks

In conclusion, the features of the tightly bound 3-boson states have been studied systematically. The universal existence of inherent nodal structures has been demonstrated analytically and numerically. The existence is irrelevant to the strength of the trap. The quantum states belonging to the same set of representations of the symmetry groups are constrained in the same way disregarding the kind of particles. Since the constraint arising from symmetry is absolutely not violable, the effect of symmetry overtakes dynamics and is decisive. In particular, there are prohibited zones (points, lines, ...) in the coordinate space not accessible to specific states. This leads to the establishment of a universal classification scheme based on the accessibility of RT, IST, and COL, and leads to the extensive similarity among different systems. Although this paper is essentially dedicated to boson systems, universality exists also in fermions systems due to the decisive role of symmetry constraint.

### Acknowledgments

The support from the NSFC under the grant No.10874249 is appreciated.

Due to having a trap, the bound states are highly localized, the above basis functions are suitable and will lead to a good convergence. Let  $N_{ab} = 2(n_a + n_b) + l_a + l_b$ . The number of basis functions is constrained by  $N_{ab} \leq N_{max}$ , the latter is given. As an example for the bosons, the

energy of the lowest  $0^+$  state with the interaction  $V_A$  would be 2.06561, 2.06558, and 2.06557  $\hbar\omega$ , respectively, if  $N_{max} = 16, 18,$  and  $20$ . Since the emphasis is placed at the qualitative aspect, the convergence appears to be satisfactory.

- 
- [1] V. Efimov, Phys. Lett. **B33**, 563 (1970).  
 [2] V. Efimov, Sov. J. Nucl. Phys. **12**, 589 (1971).  
 [3] D. E. Rutherford, Substitutional Analysis (Edinburgh University Press, Edinburgh, 1948).  
 [4] G. Racah, Group Theory and Spectroscopy (Princeton University Press, Princeton, NJ, 1951).  
 [5] E. M. Lobel, Group Theory and its Applications, Vols.1,2, and 3 (Academic Press, New York, 1968, 1971, and 1975).  
 [6] J. P. Elliott, P. G. Dawber, Symmetry in Physics, Vols.1,2 (McMillan Press, London, 1979).  
 [7] C. G. Bao, Few-Body Systems **13**, 41 (1992).  
 [8] C. G. Bao and W. F. Xie, Few-Body Systems **19**, 157 (1995).  
 [9] C. G. Bao, W. F. Xie, W. Y. Ruan, Few-Body Systems **22**, 135 (1997).  
 [10] T. Morishita and C. D. Lin, Phys. Rev. A **64**, 052502 (2001).  
 [11] M. D. Poulsen and L. B. Madsen, Phys. Rev. A **72**, 042501 (2005).  
 [12] A. R. Edmonds, Angular Momentum in Quantum Mechanics (Princeton University Press, Princeton, NJ, 1957).  
 [13] T. A. Brody and M. Moshinsk, Table of transformation Brackets (Universidad Nacional Autonoma de Mexico, Monografias del Instituto de Fisica, 1960).  
 [14] M. Baranger and K. T. R. Davies, Nucl. Phys. **79**, 403 (1966).  
 [15] W. Tobocman, Nucl. Phys. A **357**, 293 (1981).